Central Counterparty Exposure in Stressed Markets*

Wenqian Huang† Albert J. Menkveld‡ Shihao Yu§

May 6, 2019

*The authors are grateful for helpful comments from Evangelos Benos, Markus Brunnermeier, Jorge Cruz Lopez, Gerardo Ferrara, Pedro Gurrola-Perez, Mark Manning, David Murphy, Michalis Vasios, Guillaume Vuillemey, Marius Zoican, seminar participants at the Univerity of Hong Kong, and conference participants at 2015 Australasian Finance and Banking Conference, 2015 Conference on Theories and Practices of Securities and Financial Markets, 2015 SYRTO Conference on Systemic Risk, 2016 Federal Reserve International Banking Conference, and 2016 Eastern Financial Annual meeting. We thank SURFsara for the support when using the Lisa Compute Cluster. Albert and Shihao gratefully acknowledge NWO for a Vici and a Research Talent grant, respectively. Albert further thanks the Bank of Canada and the Bank of England for a week-long visit to refine his views on CCPs. The views expressed in this paper are those of the authors and do not necessarily reflect those of the Bank for International Settlements.

†Wenqian Huang, Bank for International Settlements, Centralbahnplatz 2, 4051 Basel, Switzerland, tel +41 612 808 000, wenqian.huang@bis.org.

‡Albert J. Menkveld, Vrije Universiteit Amsterdam, School of Business and Economics, De Boelelaan 1105, 1081 HV, Amsterdam, Netherlands, tel +31 20 598 6130, albertjmenkveld@gmail.com and Tinbergen Institute.

§Shihao Yu, Vrije Universiteit Amsterdam, School of Business and Economics, De Boelelaan 1105, 1081 HV, Amsterdam, Netherlands, tel +31 20 598 4722, s.yu@vu.nl.

Central Counterparty Exposure in Stressed Markets

Abstract

Time is valuable, particularly in stressed markets. As central counterparties (CCPs) have become systemically important, we need to understand the dynamics of their exposure towards clearing members *in real-time*. We track such exposure and decompose it which leads to the following insights. First, the composition of CCP exposure is fundamentally different in the tails. Second, at extreme levels or during rapid increases, there is elevated crowding. This is the result of clearing members all concentrating their positions on a single security or a particular portfolio, desirable if motivated by hedging, worrying if due to speculation.

1 Introduction

Regulators are worried about central counterparties (CCPs) risk management in fast markets. Sudden extreme price dislocations ("Flash Crashes")[1] coupled with super-human trading speeds could have systemic consequences. If traders are unable to deliver on their trades, then CCPs become liable for their losses. The (initial) margins posted by these traders might not be sufficient in which case losses are effectively mutualized. A recent example is the 2018 failure of a Nasdaq clearing member where losses swallowed up two-thirds of the default fund.[2] Such mutualized loss might itself trigger further defaults in which case the event becomes systematic.

State of the art risk management at CCPs therefore becomes of first order importance. CPMI-IOSCO (2017) emphasizes the need for monitoring intraday CCP exposure and suggests possible sources of its changes (p. 32):

> Adverse price movements, as well as participants building larger positions through new trading (and settlement of maturing trades), can rapidly increase a CCP's exposures to its participants. This exposure can relate to intraday changes in both prices and positions. For the purposes of addressing these and other forms of risk that may arise intraday, a CCP should address and monitor on an ongoing basis...

In this paper we propose a way for CCPs to monitor their exposure in real-time with a focus on stressed markets. In such markets, trading is likely to be fast paced and data therefore streams at extreme speeds. The approach should be able to cope with such "big data" challenges. More importantly, the monitoring should yield valuable economic insights that generate an understanding of "what just happened", and potentially guide interventions. This leads us to the second desirable property of a useful approach: exposure levels or changes should be accompanied by a meaningful decomposition.

We turn to the academic literature on sudden price dislocations and intense trading to find what decomposition is desirable. Several studies have identified

[1] On February 5, 2018, VIX futures jumped 20 points, which is the largest daily increase since the 1987 stock market crash. On October 7, 2016, the British pound dropped by almost ten percent in just eight minutes. On January 15, 2015, the Swiss franc rose by about 20% against the euro within five minutes after the Swiss central bank announced that it abandoned its peg against the euro as per immediately.

[2] On September 10, 2018, the Nordic-German power spread increased by more than 17 times the average daily change which triggered the trader's default.

a fire-sale channel as the root cause of price dislocations. The narrative is as follows. In normal times, arbitrageurs smooth prices by trading against pricing errors (thereby essentially engaging in market making). Suppose that at some point a critical mass of them crowds on a single risk factor. That is, their portfolio positions are very similar, say long a book-to-market or size based portfolio.[3] If this position suddenly experiences a significant loss then arbitrageurs face high variation-margin calls (to mark to market their position). If the arbitrageurs are capital constrained then they might be forced to free up capital by selling some of their position. This sell pressure might trigger trades at fire-sale prices, thus leading to more losses, triggering further selling, etc. (Shleifer and Vishny, 1997; Gromb and Vayanos, 2002; Brunnermeier and Pedersen, 2009). Perhaps the most prominent example of such dynamic is the "Quant Meltdown" where the arbitrageurs were hedge funds and the portfolios were indeed factor-based portfolios (Khandani and Lo, 2007, 2011).

With these motivations let us now discuss in more detail what we do in the remainder of the paper. We develop an approach for tracking and decomposing CCP exposure in real time, or more precisely in trade time The CCP exposure measure is based on the tail risk of losses in an oncoming period, aggregated across all clearing members (Duffie and Zhu, 2011; Menkveld, 2017).[4] The motivation behind is that a CCP essentially insures the losses in its members' portfolios and thus its exposure is commensurate to aggregate loss in the trader community.[5] The measure relies on analytic results that are all easy to compute. It further allows for decomposition across clearing members or securities.

We will implement the monitoring approach on a sample of high-frequency CCP data. We define a stressed market for a CCP by comparing the tails to the full sample.[6] The three questions we focus on are:

[3] Wagner (2011) clarifies that these arbitrageurs could hold diversified portfolios, yet be exposed to the fire-sale channel. It is position *diversity* that is the driving force here, not the level of diversification.

[4] Menkveld (2017) extends Duffie and Zhu (2011) to focus on the tail risk in losses as opposed to mean losses.

[5] The positions that a CCP observes for all its clearing members is in the securities it clears. It does not see their *net* positions as there could be partially offsetting positions in securities that it does not clear or non-traded risk that is being hedged. A prudential CCP will have to assume no offsetting positions.

[6] One could argue that the tails are not riskier to a CCP because higher exposures against clearing members are insured by the latter posting higher margins with the CCP. While this is true, it is also true that if there are losses that exceed the margin, they exceed by a larger amount in the tail (i.e., loss given default is likely to be larger). A deeper analysis of risk net of margin and other

1. Are sudden extreme increases in CCP exposure driven by the same factors as regular exposure changes? Or does one see, for example, elevated crowding?

2. Is the same true for extreme *levels* as opposed to extreme *changes*? Again, is crowding a larger part of it?

3. Finally, at these extreme levels is the relative contribution of clearing-member house accounts larger than their for-client accounts? If so, then this is worrisome as clearing members are typically highly leveraged financial intermediaries and therefore have less ability to absorb large shocks.

The answers are based on a high-frequency analysis of a 2009-2010 sample of a European CCP. Time runs in volume buckets of about fifteen minutes. The CCP was the largest equity CCP in Europe and later merged with DTCC in the US to become the world's largest equity CCP. Counterparty risk arises in equity CCPs as settlement of a trade typically occurs three days after a trade is concluded. A trade therefore is like a three-day forward contract between the two sides to a trade. Counterparty risk then pertains to one side defaulting in this period. Admittedly, analysis of a CCP that insures credit-default swaps or interest-rate swaps would have been more relevant in terms of systemic risk, but disaggregated CCP data is extremely hard to come by (see literature review below). The application to actual CCP data could therefore in and of itself be considered a contribution.

The key empirical findings are several. First, while average CCP exposure changes are almost entirely driven by position changes of clearing members, when zooming in on the extreme exposure changes, security volatility and position crowding start to contribute substantially. For the top 100 changes they collectively contribute about 20%, rising to almost 50% for the top 10 changes. In the latter case, volatility contributes about 30% and crowding about 20%.

Second, a similar finding pertains when decomposing CCP exposures and comparing extreme *levels* of CCP exposure to the rest of the sample. There turns out to be more crowding at these times too. More specifically, CCP exposure starts to concentrate with a few clearing members on a smaller set of risk factors. Comparing the full sample with the top one percent in terms of exposure level, the contribution of the largest five members increases from 29% to 47%. The contribution of the largest principal component across all risk factors increases from 7% to 42%.

forms of collateralization (e.g., the default fund) are beyond the scope of this study.

Third, it is not true that relative more of the CCP exposure resides in house accounts at extreme levels. There is only a modest increase from 67% to 70% when comparing the full sample to the top 1%. However, it is true that this total contribution resides with fewer clearing members. In other words, CCP exposure concentrates on fewer clearing members' house accounts which in of itself is a cause of concern. If there is an adverse price shock in this case, the CCP needs to impose extreme variation-margin calls on a few highly-leveraged institutions.

In sum, the findings collectively suggest that there is concentration of risk both for rapid exposure increases and at extreme exposure levels. In the latter case, the crowding is driven both by fewer clearing members taking larger position on fewer risk factors. The same is observed if one zooms in on house-accounts only, more concentration. This elevated crowding on all these dimensions raises the risk of negative price spirals potentially triggering multiple defaults as emphasized in fire-sale literature.

One additional finding worth emphasizing here is that idiosyncratic events can have large effects on CCP exposure. An example in our sample is a disappointing earnings announcement by Nokia at noon on April 22, 2010, which caused its share price to fall by about 15% in the minutes after and volume jumped and stayed at an elevated levels throughout the afternoon. Real-time exposure analysis reveals that the immediate steep exposure jump was due to volatility. This jump however was only a relatively small part of the extremely large CCP exposure increase that day. Most of it was due to rapid position expansion through lots of trading that afternoon. (Note that this is a non-trivial finding as the heavy volume could have been due to traders reducing their positions after observing elevated volatility.[7]) Finally, the contribution of the crowding component that day is positive — not surprisingly the crowding that day was in the Nokia stock. In summary, a CCP risk manager should be focused not only on macro news, but also on security-specific news as it can trigger active position taking (potentially speculation) which is potentially toxic when combined with a volatility spike and position crowding.

Our paper contributes to a rapidly expanding empirical literature on central clearing. CCP trade data disaggregated across members are scarce. Proprietary daily data have been used to compare CCP exposure to the margins that were collected (Jones and Perignon, 2013; Menkveld, 2017; Cruz Lopez et al., 2016).

[7] Bignon and Vuillemey (2016, Fig. 3 and A1) do a forensic analysis on the Paris commodity futures CCP that failed in 1974. They, for example, find that there was elevated activity (in terms of transactions) in the half year before failure, but open positions declined (measured in 1000 tons sugur).

Duffie, Scheicher, and Vuillemey (2015) analyze a snapshot of bilateral exposures on uncleared credit default swaps to assess the netting efficiency potential of central clearing. Event studies on CCP introductions yield insight in how trading is affected (Loon and Zhong, 2014, 2016; Menkveld, Pagnotta, and Zoican, 2015; Benos, Payne, and Vasios, 2016). We contribute to this literature by proposing a feasible approach to CCP exposure changes in real time and offers an economically meaningful decomposition.

The paper further contributes to a nascent literature on CCP systemic risk. Capponi, Cheng, and Rajan (2014) analyze the endogenous build-up of asset concentration due to central clearing. Amini, Filipović, and Minca (2015) investigate partial netting for a subset of liabilities in a network setting that accounts for knock-on effects and asset liquidation effects. Glasserman, Moallemi, and Yuan (2015) compare margining in dealer markets and a centrally cleared market. Menkveld (2016) endogenizes the fire sale premium that a CCP will have to pay in the catastrophic state that a critical mass of members default and liquidity supply is thus impaired.[8]

The rest of the paper is organized as follows. Section 2 formalizes and motivates the three overriding hypotheses. Section 3 presents the approach to monitoring and decomposing CCP exposure. Section 4 describes the data and discusses implementation issues. Section 5 presents the empirical results of testing the three hypotheses. Section 6 concludes.

2 Hypotheses

This section develops three hypotheses that will be taken to the data. Each hypothesis is stated formally and then followed by a motivation.

Hypothesis 1. *The drivers of CCP exposure* changes *are different in the (right) tail.*

CCP exposure changes can be driven by a variety of factors that are either price related (e.g., volatility or correlation) or trade related (i.e., trade causes member positions to change). We expect the latter to dominate CCP exposure changes at normal times. However, we conjecture that turbulent periods are characterized by elevated volatility and lots of trading. The strong positive correlation of volatility

[8] A related set of papers does not focus on concentration and systemic risk but rather on incentives and economic efficiency Koeppl, Monnet, and Temzelides (2012); Fontaine, Perez-Saiz, and Slive (2014); Acharya and Bisin (2014); Biais, Heider, and Hoerova (2016); Huang (2019).

and transaction rate is a well-known stylized fact in the microstructure literature (e.g., Jones, Kaul, and Lipson, 1994).

The intense trading at times of extremely high volatility does *not* necessarily imply that CCP exposure increases rapidly. A sudden volatility increase might actually trigger traders to *reduce* their recently established positions to contain risk. Such trading benefits a CCP as it dampens its exposure increase or could even reduce it in extreme cases.

On the other hand, such volatility shock might lead to (more) speculation in which case traders increase their positions in magnitude. A heterogeneity in beliefs or signals might generate such stronger position taking (e.g., Kim and Verrecchia, 1994). Or, in a more recent paper, Crego (2019) proposes a channel by which risk-averse traders strategically wait with trading on their private signal until after the arrival of a public signal that removes significant uncertainty. Either way, member positions would increase in magnitude and CCP exposure rapidly increases as a result.

An even more worrisome channel that could cause high volatility and fast trading is what, in the literature, is often called a self-reinforcing fire-sale channel. For example, financially constrained arbitrageurs (hedge funds, sell-side banks, etc.) hit by adverse-price shocks might have to quickly liquidate their large positions and thereby cause transitory price shocks (Shleifer and Vishny, 1997; Gromb and Vayanos, 2002; Brunnermeier and Pedersen, 2009). It would not be a concern if their positions were diverse (Wagner, 2011). However, arbitrageurs might have followed similar trading strategies and entered into the same positions (Stein, 2009). As a result, their portfolio returns will be high correlated since the positions to be liquidated crowd on a single risk factor (e.g., a security or a particular portfolio). In this case, there might not be enough cash-in-the-market in which case markets have to clear at fire-sale prices. A prominent example is the "Quant Meltdown" of 2007 when quantitative equity market-neutral hedge funds crowded on similar trading strategies and made record losses (Khandani and Lo, 2007, 2011). This risk that the CCP finds itself in this scenario is particularly high when there is substantial crowding in clearing members' portfolios.

In sum, testing the hypothesis in the data requires one to decompose CCP exposure changes into, at the minimum, price- and trade-related components whereby one of the trade-related components should be crowding across clearing members. It will then be possible to study whether or not members engage relatively more in expanding their positions and crowding on a particular risk factor.

Hypothesis 2. *The structure of CCP exposure* levels *is different in the (right) tail.*

Hypothesis 2 restates Hypothesis 1 but this time in terms of *levels* instead of *changes*. The reason to also study whether there is, for example, elevated crowding for extreme levels is derived from studies on historical CCP failures. Bignon and Vuillemey (2016) study the 1974 failure of the Paris Commodity Clearing House. They show that in a year starting from November 1973 the position of the largest clearing member rose from 9% of the total open position in sugar futures to 56% of it. Another example is the 1987 failure of the Hong Kong Futures Guarantee Corporation where at the point of failure the largest five members had accumulated 80% of the short position in all contracts (IMF, 2010).

To fully understand the source of crowding the monitoring approach should allow for both decomposing the exposure *level* across clearing members, but also across risk factors. The reason is that strong crowding could occur because outstanding positions are held by only a few clearing members. The CCP failures in Paris and Hong Kong are examples of such crowding. There is however a more opaque way for there to be elevated crowding. In the extreme case, all clearing members share an equal position but they crowd on a single risk factor, for example one security or a particular portfolio. The 2007 Quant Crisis is an example of position crowding. Let us turn to a simple example to clarify the difference.

Suppose there are four clearing members and two equal assets with orthogonal payoff. First consider the baseline case of member 1 and member 2 having traded asset A and therefore have open and opposite positions in this asset. Suppose the same holds for member 3 and 4 in asset B. In this baseline case there is no crowding. Let us now consider the two polar cases of crowding. An example of perfect *member* crowding is one where member 1 and 2 trade as in the baseline case, but member 3 and 4 refrain from trading. An example of perfect *position* crowding is again the baseline case, but now member 3 and 4 also trade asset A. Note that in this case all clearing members have an equal position, yet there is perfect crowding.

When testing the second hypothesis, it is desirable to not only measure the level of crowding but also identify whether it is member or position crowding. These properties will be discussed in more detail when presenting the monitoring approach in Section 3.3.

Hypothesis 3. *The relative contribution of house accounts to CCP exposure increases in the (right) tail.*

The third hypothesis is focused on distinguishing clearing-member house and client accounts. House accounts capture the trading that clearing members do for their own books whereas in client accounts they register their trading on behalf of

clients. It is worth decomposing CCP exposure across these two types of accounts as one could argue that CCP exposure to house accounts carries more risk. Clearing members are often highly leveraged financial intermediaries whose trading is unlikely to be pure hedging. For example, they often engage in market making to absorb temporary order imbalance. Therefore relatively more exposure to house accounts at times of high CCP exposure is likely to be worrisome. Testing the third hypothesis will show whether or not this is the case.

3 Approach

This section presents an approach to monitoring CCP exposure in real time. It is based on the framework proposed by Duffie and Zhu (2011) and extended by Menkveld (2017) to include tail risk and crowding. CCP exposure is essentially a measure that is based on the distribution of losses in clearing member accounts for the oncoming period. We study the Value at Risk (VaR) for these losses following Menkveld (2017).[9] We first present the exposure measure in detail, then show how one could decompose exposure changes needed for testing the first hypothesis, and finally present exposure level decompositions needed for the second and third hypothesis.

3.1 The CCP exposure measure: A VaR of aggregate loss

Consider the case of a single CCP, I securities, and J clearing members (or traders, the two are used interchangeably below). P_t is an $I \times 1$ vector consisting of current security prices and R_t is an $I \times 1$ vector that contains next period's security returns. R_t is assumed to be normally distributed[10]: $R_t \sim \mathbf{N}(0, \Omega_t)$ where Ω_t is the $I \times I$ covariance matrix of security returns. Let $n_{j,t}$ be an $I \times 1$ vector that captures a member's current dollar positions. The dollar portfolio return for a member in the next period is then a scalar $X_{j,t}$ where $X_{j,t} = n'_{j,t} R_t$.

Collect all $n_{j,t}$ into an $I \times J$ matrix N_t which thus becomes the dollar position matrix of all members. Collect all $X_{j,t}$ into the $J \times 1$ vector X_t which thus becomes the future return vector for all members, where $X_t = N'_t R_t$. Since X_t is linear in R_t,

[9] Duffie and Zhu (2011) study the *mean* loss which is invariant to the level of crowding — the VaR loss is not.

[10] The normality assumption yields analytic results and complete level decompositions. To stay close to normality in the data, the clock will runs in transaction time. Details are in Section 4.2.

X_t is normally distributed: $X_t \sim \mathbf{N}(0, \Sigma_t)$ where $\Sigma_t = N_t' \Omega_t N_t$ is the $J \times J$ covariance matrix of portfolio returns.

As a CCP is exposed to losses, define

$$L_{j,t} = -\min\left(0, X_{j,t}\right) \tag{1}$$

as the loss in member j's portfolio. Then the aggregate loss A in the member community is:

$$A_t = \sum_j L_{j,t}. \tag{2}$$

Duffie and Zhu (2011) propose to base CCP exposure on the *mean* aggregate loss:

$$\mathrm{E}\left(A_t\right) \tag{3}$$

and derive an analytical expression for it, which suffices for their analysis of netting efficiency, Menkveld (2017) considers the VaR of aggregate loss a better measure for CCP risk management and coins it as *ExpCCP* which is the measure we will use as well. Following standard practice and to maintain tractability, Menkveld uses the delta-normal method to compute VaR:

$$ExpCCP_t \equiv \mathrm{VaR}(A_t) = \mathrm{E}(A_t) + \alpha \mathrm{var}(A_t)^{\frac{1}{2}} \tag{4}$$

where α is a parameter to needs to be calibrated (as will be done in Section 4.2).

Let L_t be the $J \times 1$ vector that stacks all $L_{j,t}$. Since $A_t = \sum_j L_{j,t}$, one needs to compute $\mathrm{E}(L_t)$ and $\mathrm{var}(L_t)$ to evaluate (4). Following Menkveld (2017, Proposition 1) yields the following two results:

$$\begin{aligned} \mathrm{E}(L_t) = \mu_t, \quad \mu_{j,t} &= \sqrt{\frac{1}{2\pi}}\sigma_{j,t}, \\ \mathrm{var}(L_t) = \Psi_t, \quad \psi_{ij,t} &= \frac{\pi - 1}{2\pi}\sigma_{i,t}\sigma_{j,t} M\left(\rho_{ij,t}\right), \end{aligned} \tag{5}$$

where $\sigma_{ij,t}$ is the (i, j)-th element of the covariance matrix of member portfolio returns Σ_t, $\sigma_{i,t}$ is short for $\sigma_{ii,t}^{\frac{1}{2}}$, and $\rho_{ij,t} = \sigma_{ij,t}/\sigma_{i,t}\sigma_{j,t}$. The function

$$M(\rho) = \left[\left(\frac{1}{2}\pi + \arcsin\left(\rho\right)\right)\rho + \sqrt{1-\rho^2} - 1\right] / \left(\pi - 1\right) \tag{6}$$

maps portfolio return correlations into portfolio loss correlations. Detailed proofs are in Menkveld (2017). *ExpCCP* can now be written explicitly as:

$$ExpCCP_t = \sum_j \sqrt{\frac{1}{2\pi}}\sigma_{j,t} + \alpha\left(\sum_i \sum_j \frac{\pi - 1}{2\pi}\sigma_{i,t}\sigma_{j,t} M\left(\rho_{ij,t}\right)\right)^{\frac{1}{2}}. \tag{7}$$

3.2 Decomposition of CCP exposure change

The first hypothesis states that the drivers of CCP exposure changes are different in the tail. As discussed in the hypothesis section, sudden extreme CCP exposure increases might be driven by volatility shocks and crowding in addition to position changes. To test such hypothesis one needs to decompose exposure changes and verify to what extent volatility and crowding contribute a larger part in the tail.

We propose to decompose exposure changes based on a relatively straightforward one-factor-at-a-time (OFAT) analysis (Daniel, 1973). The underlying factors will consist of price-related factors such as security volatility, correlation, and price levels and trade-related factors such as member positions *per se* and crowding in positions across members. The remainder of this subsection describes the approach in detail.

Let us start by writing $ExpCCP_t$ as defined in (4) as a function of the underlying variables:

$$ExpCCP_t = f(\Sigma_t). \tag{8}$$

To arrive at a meaningful decomposition across factors we use the following two insights:

1. Following the financial econometrics literature we decompose covariance matrices into their diagonal and off-diagonal components as follows (Bollerslev, 1990; Engle, 2002):

$$\Psi_t = D_{\Psi_t} R_{\Psi_t} D_{\Psi_t}, \tag{9}$$

   where D_{Ψ_t} is a diagonal matrix with $\psi_{ii,t}$ as the i-th diagonal element and R_{Ψ_t} is the correlation matrix associated with the covariance matrix Ψ_t. This decomposition will turn out to be useful to identify correlation effects in security returns and crowding in portfolio positions.

2. Σ_t is itself a function of "deeper" variables:

$$\begin{aligned} ExpCCP_t &= f(\Sigma_t) \\ &= f(N_t \Omega_t N_t') \\ &= f\left(\Omega_t, P_t, \tilde{N}_t\right) \end{aligned} \tag{10}$$

   where the variables are: the covariance matrix of security returns Ω_t, the price level P_t, and the member portfolio holdings' matrix $\tilde{N}_t$ expressed in terms of the number of securities (as opposed to N_t which is expressed in

dollars). The reason for using $\tilde{N}_t$ is to be able to pull out a price-level effect when considering the change from N_{t-1} to N_t.

Combining (9) and (10) yields:

$$\begin{aligned} ExpCCP_t &= f(\Sigma_t) \\ &= f(D_{\Sigma_t} R_{\Sigma_t} D_{\Sigma_t}) \\ &= f\left(D_{\Sigma_t}\left(D_{\Omega_t}, R_{\Omega_t}, P_t, \tilde{N}_t\right), R_{\Sigma_t}\left(D_{\Omega_t}, R_{\Omega_t}, P_t, \tilde{N}_t\right)\right), \end{aligned} \tag{11}$$

which expresses $ExpCCP_t$ in terms of price-related variables (D_{Ω_t}, R_{Ω_t}, P_t) and trade-related variables ($\tilde{N}_t$). The OFAT decomposition changes these variables sequentially from their $t-1$ value to their value at t. The sequencing matters and we pick the baseline sequencing according to the following principles:

- Price variables change first, followed by trade variables. The reason for this sequencing is that it identifies a "pure" price effect. In other words, the price components communicate what CCP exposure change would have been had member portfolio not changed.
- Changes in idiosyncratic volatilities precede changes in correlations. In other words, we first consider changes in the diagonal and then changes in the off-diagonal of a covariance matrix. This approach makes interpretation of the components straightforward: Changes in variances become pure in the sense that they are evaluated keeping correlations constant. Interaction effects due to correlation-changes all enter the correlations component.

These principles therefore suggest the following baseline OFAT decomposition

$$\begin{aligned} \Delta ExpCCP_t =& f\left(D_\Sigma\left(\overset{1}{D}_{\Omega_t}, \overset{2}{R}_{\Omega_t}, \overset{3}{P}_t, \overset{4}{\tilde{N}}_t\right), R_\Sigma\left(\overset{1}{D}_{\Omega_t}, \overset{2}{R}_{\Omega_t}, \overset{3}{P}_t, \overset{5}{\tilde{N}}_t\right)\right) \\ & - f\left(D_\Sigma\left(D_{\Omega_{t-1}}, R_{\Omega_{t-1}}, P_{t-1}, \tilde{N}_{t-1}\right), R_\Sigma\left(D_{\Omega_{t-1}}, R_{\Omega_{t-1}}, P_{t-1}, \tilde{N}_{t-1}\right)\right). \end{aligned} \tag{12}$$

where the sequencing is illustrated by the (red) numbers on top of the various variables.[11] The decomposition yields five components. For example, the first

[11] As a robustness check, we consider 24 different sequential orders in total (see Section 5.1 and Appendix D.1).

component $RetVola_t$ is computed as:[12]

$$\begin{aligned} RetVola_t = & f\left(D_\Sigma\left(\boldsymbol{D_{\Omega_t}}, R_{\Omega_{t-1}}, P_{t-1}, \tilde{N}_{t-1}\right), R_\Sigma\left(\boldsymbol{D_{\Omega_t}}, R_{\Omega_{t-1}}, P_{t-1}, \tilde{N}_{t-1}\right)\right) \\ & - f\left(D_\Sigma\left(D_{\Omega_{t-1}}, R_{\Omega_{t-1}}, P_{t-1}, \tilde{N}_{t-1}\right), R_\Sigma\left(D_{\Omega_{t-1}}, R_{\Omega_{t-1}}, P_{t-1}, \tilde{N}_{t-1}\right)\right). \end{aligned} \tag{13}$$

which captures the contribution of volatility change.

We list the five components below and discuss each of them in detail. Note that the numbering corresponds to the red numbers in (12)):

Price components.

1. *RetVola*: The impact of the change in the volatility security returns on CCP exposure change. This effect captures the well-known empirical fact that volatility is time-varying (commonly referred to as "GARCH" or "stochastic volatility" in the financial econometrics literature).

2. *RetCorr*: The additional impact of a change in the *correlations* of security returns on CCP exposure change. The time-varying nature of such correlations is another well known empirical fact and can be identified, for instance, through a dynamic conditional correlation (DCC) model (Engle, 2002). The impact of changing correlations is particularly important for sudden steep drops in security prices. Not only does volatility increase in such events, correlations also tend to increase (Preis et al., 2012). This interaction effect is, by first considering volatilities and then correlations in the decomposition, completely assigned to *RetCorr*.

3. *PrLevel*: The additional impact of a change in the price level of securities. This effect is entirely due to covariance matrices being defined in relative terms (i.e., it is based on percentage returns as opposed to dollar returns). For example, a covariance matrix might not have changed in the interval, but if price levels dropped, then CCP exposure dropped because the latter is defined in terms of dollars. Such effect is picked up by *PrLevel*.

Trade components.

4. *TrPosition*: The additional impact of new trades that arrived in the interval. These trades might expand or reduce traders' legacy positions. CCP exposure therefore does not necessarily increase after new trades. It declines if their overriding effect was to reduce traders' positions.

[12] We include explicit formulas for all five components in Appendix A for completeness.

5. *TrCrowding*: The additional effect due to a change in the extent to which the returns in member portfolios correlate. If such correlations increased as a result of the new trades, then CCP exposure increased. This effect is referred to as crowding as increased correlations imply that the new trades tilted member portfolios towards common risk factors.

In Appendix B we illustrate the decomposition of exposure changes by presenting a simple example. We discuss how the various components change when changing either price- or trade-related variables.

3.3 Decomposition of CCP exposure level

Testing the second and third hypothesis requires a decomposition of CCP exposure level (as opposed to exposure change). To test whether there is more crowding at higher exposure levels, it is desirable to decompose CCP exposure level across members and across securities. If one finds more concentration either across members or across securities, then there is elevated crowding as discussed in Section 2.

Homogeneity of degree one suggests a natural decomposition of level both across members and across securities. Let us focus on the decomposition across members (Menkveld, 2017, Section 1.5). As *ExpCCP* is homogeneous in risk of individual members (i.e., σ_j), applying Euler's homogeneous function theorem yields:[13]

$$ExpCCP = \sum_j \sigma_j \left(\frac{\partial}{\partial \sigma_j} ExpCCP \right). \tag{14}$$

The contribution of member j therefore is:[14]

$$\begin{aligned} ExpCCP_j &= \sigma_j \left(\frac{\partial}{\partial \sigma_j} ExpCCP \right) \\ &= \sqrt{\frac{1}{2\pi}} \sigma_j + \sum_{i \in \{J\}} \frac{\alpha}{\text{std}A} \left(\frac{\pi - 1}{2\pi} \right) \sigma_i \sigma_j M(\rho_{ij}), \end{aligned} \tag{15}$$

where

$$M'\left(\rho_{ij}\right) = \frac{\frac{1}{2}\pi + \arcsin\left(\rho_{ij}\right)}{\pi - 1}. \tag{16}$$

[13] Time subscripts are suppressed here for the sake of brevity.

[14] This equation corresponds to Menkveld (2017, equation (27)). Note that there is typo in (27) as $\sqrt{1/(2\pi)}$ should have been multiplied by σ_j instead of σ_j^2. This typo has been corrected in (15) below.

Verbally this results suggest that member j's contribution to *ExpCCP* is equal to its level of risk (i.e., σ_j) multiplied by the (marginal) price of such risk in terms of CCP exposure (i.e., $\frac{\partial}{\partial \sigma_j} ExpCCP$).

A decomposition across securities is derived analogously where the risk units are ω_k instead of σ_j. The detailed derivation is included as Appendix C.

4 Application

This intermezzo section presents the data and discusses various implementation issues. These issues include whether returns are normally distributed (needed for *ExpCCP*), estimating the return covariance matrix, and picking the parameter α in the delta-normal VaR to arrive at a standard 1% exceedance rate.

The data sample used in the application was made available to us by the European Multilateral Clearing Facility (EMCF). EMCF, now merged with DTCC in the U.S. to become EuroCCP, is an equity CCP for Nordic stock markets, including Denmark, Finland, and Sweden. The sample consists of trade reports with time stamp, size, price, anonymous counterparty ID and whether the trade was done on a member's house account or a client account. A trade done on a house account is for a clearing member's own book whereas a client account is trade done for clients.[15] The data sample runs from October 19, 2009, through September 10, 2010, and includes trades on almost all exchanges: NASDAQ-OMX, Chi-X, Bats, Burgundy, and Quote MTF. The only exchange whose Nordic trades it did not clear was Turquoise. Turquoise, however, had a market share of less than 1% at the time.

An equity CCP insures counterparty risk for equity trades in the period that starts when a trade is concluded and ends when it settles. When an exchange concludes a trade, the money and the securities are not immediately transferred. Such transfer happens three days later in our sample. Should one side to the trade default in this period, the CCP inherits its position and the trade will follow through all the way to settlement.

A three-day deferred settlement is conceptually similar to a three-day forward contract between the two sides of the trade. To fix language, we therefore refer to yet to settle trades as "positions." Note that these positions change overnight absent any trade. This change is simply due to settlement of legacy trades and these

[15] The new post-crisis EMIR regulation in Europe requires a CCP to segregate trades on house accounts from those on client accounts as of 2013. Our data sample precedes this date but EMCF had already implemented such segregation.

Table 1: Summary statistics. This table presents various summary statistics for the CCP data sample. Trades on house accounts are for a clearing members' own book, whereas client accounts refer to trading they do for clients.

Panel A: General information

Number of trading days		228
Number of stocks		242
	House accounts	87
Number of members	Client accounts	139
	Total	226

Panel B: Trade information across stocks

	Mean	Std. Dev.	Median
Mean of daily number of trades	590	1,056	102
Mean of daily volume (shares)	398,922	1,074,108	33,143
Mean of daily volume (euro)	4,521,293	9,767,987	371,674

Panel C: Trade information across clearing members (by account type)

	All accounts	House accounts	Client accounts
Mean of daily volume (shares)	1,207,610	1,577,985	819,003
Std of daily volume (shares)	2,259,359	2,747,832	1,497,918
Within member std of daily volume (shares)	879,348	1,261,212	627,665
Mean of end-of-day position (euro)	0	-11,237	11,567
Std of end-of-day position (euro)	1,535,067	1,880,137	1,069,244
Within member std of end-of-day position (euro)	619,105	988,685	387,785

trades are therefore removed from traders' positions. In other words, if a trader does not trade for three consecutive days, his position in all equities becomes zero as all his earlier trades settled. Finally, we refer to a trader's set of open positions at any point in time as his portfolio. We emphasize that this is not be confused with a trader's portfolio in terms of the equity he is holding. It simply refers to the yet to settle trades as these are relevant for CCP exposure since it is for these open positions that the CCP insures counterparty risk.

4.1 Data

Summary statistics. Table 1 introduces the sample by presenting various summary statistics. The sample captures trading in 242 stocks on 228 days. It contains 226 trading accounts, 87 of which are house accounts and the other 139 are client accounts.

Disaggregating trades across securities shows that the stocks are reasonably actively traded. On average a stock trades 590 times per day generating an average

volume of 4.5 million euro. The corresponding standard deviations are 1,056 and 9.8 million, respectively, thus showing there is considerable variations in the sample.

Disaggregating trades and positions across member-house and member-client accounts yields the following insights. For all accounts, the average daily volume is 1.2 million shares, with a standard deviation of 2.3 million shares. The overall average position is zero because for every buyer there is a seller. The overall standard deviation of position is €1.5 million. The within (account) standard deviation of both volume and position is relatively modest. In other words, most variation of volume and position is across accounts, but there also is substantial through-time variation in accounts (at least a third of overall variation).

Separating house and client accounts, one observes that house accounts trade more actively than client accounts. The average daily volume on house accounts is 1.6 million shares, twice as large as volume on client accounts. The standard deviation of house volume is 2.7 million shares, again substantially higher than the standard deviation of client volume which is 1.5 million shares. House accounts also have larger variation in terms of position. The standard deviation of house position is €1.9 million whereas the standard deviation of client position is €1.1 million.

4.2 Implementation issues

Volume clock with aim to recover normally distributed returns. It is well known that financial returns are not normally distributed when measured on a wall clock. Returns exhibit negative skewness and excess kurtosis, especially at high frequencies. However, the financial-econometrics/microstructure literature has shown that normality of security returns can be recovered when time is measured on a volume-clock as opposed to the wall-clock (Clark (1973); Ané and Geman (2000); Easley, López de Prado, and O'Hara (2012)). When using a volume clock security prices are sampled each time a pre-specified amount of volume has been traded. It turns out that taking log differences of such prices is much closer to normal with less negative skewness and excess kurtosis.

As normally distributed portfolio returns are important for computing *ExpCCP*, we will use a volume-clock in our application inspired by Easley, López de Prado, and O'Hara (2012).[16] We pick the average number of volume bins per day to

[16]More specifically, the conversion of portfolio-return correlations to portfolio-loss correlations is done with the M function in (16) which relies on normality.

be equal to 34. This corresponds to a 15-minute frequency on the wall clock as the market is open from 9:00 to 17:30. The bin size therefore is picked to be the average daily market volume in terms of shares divided by 34. The choice for a 15-minute frequency is common in the microstructure literature as it strikes a balance between sample size and microstructure noise (Hansen and Lunde, 2006). As a robustness check, we consider other frequencies as well (see Section 5.1 and Appendix D.3).

Our implementation follows the extant volume-clock literature except for two notable differences. First, instead of creating a clock security by security based on security-specific trading, we group all securities together and implement the clock on the group. Suppose the clock starts now, then the latest prices known now are stacked into a vector. If the volume bin is one million shares, then we wait until one million shares were traded *across* all securities, and then again stack the latest prices of all securities into a vector. Returns then are obtained through standard log differencing. The benefit of this approach is that we have a unified (market) volume-clock.

Second, ideally trades should be grouped only by volume, completely ignoring wall-clock time. However, in order to accommodate the settlement of legacy trades at the end of each day, we group trades intra-daily for each day separately.[17]

To assess whether the volume-clock delivers closer to normally distributed returns than the wall-clock, we compute both based on member portfolio dollar returns. Wall-clock returns are based on 15-minute intervals. Table 2 presents skewness of returns, their excess kurtosis, and the Jarque-Bera statistic which includes both skewness and kurtosis. Under the null of normality, these statistics are all zero in expectation. Return statistics are presented individually for the largest five clearing members in terms of volume, for all them pooled, and for all members pooled.

The results show strong evidence in favor of the volume-clock when returns are required to be normal. All three statistics are substantially smaller in magnitude for all five members. When pooled, skewness drops from 0.96 to 0.07, kurtosis drops from 46.13 to 3.15, and the Jarque-Bera statistic drops from 92.11 to 0.69. For *all* clearing members pooled, skewness decreases in magnitude from -0.61 to -0.21, kurtosis drops from 199.91 to 31.86, and Jarque-Bera drops from 1709.43 to 32.25. These statistics suggest that non-normality is much less of an issue for the volume-clock consistent with earlier literature.

[17] In case of any residual trades due to imperfect grouping, they are included in the last bin of each day.

Table 2: Statistics on member portfolio returns: Wall- versus volume-clock. This table presents various statistics on realized dollar returns on member portfolios. These statistics are presented for wall-clock and volume-clock returns to assess to what extent the returns are normally distributed. The statistics include skewness, excess kurtosis, and the Jarque-Bera statistic. The latter combines the former to and is computed as $(S^2 + K^2/4)/6$, where S is the skewness and K is the excess kurtosis. The clock runs in 15-minute intervals for the wall-clock and for a bin size that, on average, makes a volume bin last 15 minutes. Statistics are presented for the largest five members in terms of volume, for them pooled, and for all members pooled.

	Skewness		Kurtosis		Jarque-Bera	
Member	Wall-clock	Volume-clock	Wall-clock	Volume-clock	Wall-clock	Volume-clock
Largest	-0.29	-0.15	8.69	3.23	3.16	0.44
2nd largest	1.47	0.00	30.04	4.75	37.96	0.94
3rd largest	1.76	0.11	107.78	2.24	484.52	0.21
4th largest	-0.46	0.10	15.73	1.33	10.35	0.08
5th largest	1.97	0.28	46.85	4.04	92.11	0.69
Largest 5 pooled	0.96	0.07	46.13	3.15	88.82	0.41
All pooled	-0.61	-0.21	202.55	27.82	1709.43	32.25

Estimate the time-varying return covariance matrix. To account for time-varying volatility in returns, we estimate Ω_t as the exponentially weighted moving average (EWMA) of the outer product of returns. This follows standard practice (e.g., RiskMetrics and EMCF) and corresponds to estimating an IGARCH(1,1).

What remains is to pick the EWMA decay parameter. RiskMetrics uses 0.94 when implementing their estimate on their highest frequency: daily data. As round-the-clock variance is 47 times the intraday 15-minute variance[18] we pick the decay parameter to be 0.9987 as $0.9987^{47} = 0.94$. Ω_t is therefore calculated recursively as:[19]

$$\Omega_t = (1 - 0.9987)R_{t-1}R'_{t-1} + 0.9987\Omega_{t-1}. \tag{17}$$

The sample we use for analyzing CCP exposure starts on December 7, 2009, but we use data as of October 19 that year to have a burn-in period for Ω_t. We start the recursion off with the zero matrix, but given that 0.94 corresponds to a half-life of 11 days, the effect of this choice is negligible by the time we arrive at

[18]Note that as the trading period contains 34 15-minute intervals, this implies that the variance of overnight returns corresponds to about the variance of 47-34=13 intraday 15 minute intervals.

[19]Given that the overnight period in terms of volatility corresponds to five 15-minute intervals, we update the covariance matrix when encountering an overnight return R_{t-1} by $\Omega_t = (1 - 0.9987^5)\tilde{R}_{t-1}\tilde{R}'_{t-1} + 0.9987^5\Omega_{t-1}$ where $\tilde{R}_{t-1} = R_{t-1}/\sqrt{5}$.

December 7, 2009. As robustness check, we use a rolling-window estimate of the covariance matrix and the results do not change qualitatively (see Section 5.1 and Appendix D.2).

Pick α to make *ExpCCP* a 99% VaR. CPMI-IOSCO (2012) recommends that a CCP use a 99% VaR to set margins. We follow this lead and calibrate the alpha parameter in our delta-normal VaR to 2.5 to achieve an exceedance rate of 1%.[20]

5 Results

This section starts with presenting the time series of CCP exposure levels and changes. Several salient spikes will be discussed. It is followed by three subsections in which the three hypotheses of Section 2 are tested.

Figure 1 plots the CCP exposure measure *ExpCCP* for all volume bins in the sample. The top graph plots its level throughout the sample and reveals one salient large spike in May 2010. This turns out to be the peak month in the Greek sovereign wealth crisis.[21] *ExpCCP* reached €8 million which is the 99% VaR of losses across all members in the oncoming volume bin. Although such level is about triple the average level, it still is a relatively moderate amount and will not cause a systemic crisis in and of itself. As stated in the introduction, equity CCPs are unlikely to be systemic but as CCP data is extremely scarce we are blessed to have such data. We believe it is interesting to study the dynamics (which is what we do in the remainder of the section) to test several hypotheses. We hope future research will benefit from derivative CCP data.

High levels of CCP exposure in *Nordic* equity markets during the *Greek* sovereign debt crisis might sound surprising. It is however not that surprising given the literature on this crisis. For example, Mink and De Haan (2013) find that news about the Greek bailout generally led to abnormal stock returns for European (including Nordic) banks: Positive returns for regulatory initiatives that favor banks, negative

[20] Note that aggregate loss is not normal since it is the sum of *truncated* normals and therefore not normal.

[21] A review of the main events in this month is as follows. On May 5 mass protests erupted in Greece against the imposed austerity measures, with three deaths reported. This social unrest led to concerns that it could jeopardize the rescue package proposed by the European Union and the International Monetary Fund on May 2. To fund this intervention and future ones, the European Commission created the European Financial Stabilisation Mechanism on May 9 (EC, 2010). On May 10, the European Central Bank announced the Securities Markets Program to address "dysfunctional" securities markets (ECB, 2010).

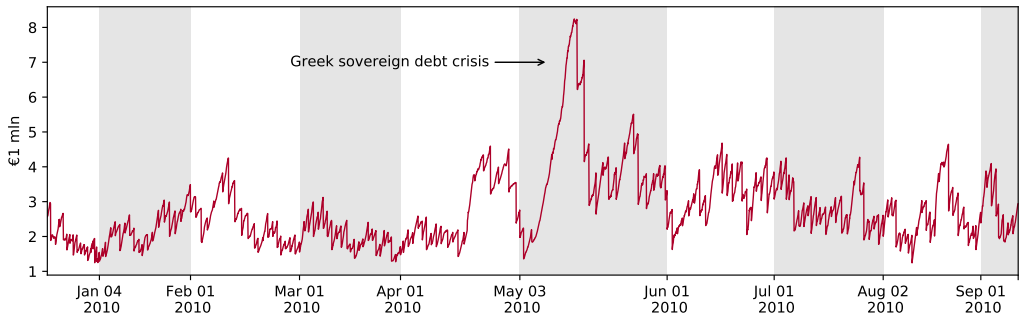

(a) CCP exposure level

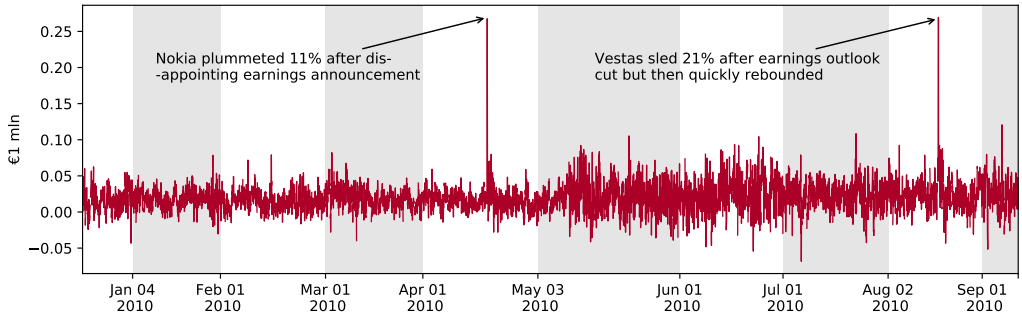

(b) CCP exposure change

Figure 1: CCP exposure level and change. This figure plots CCP exposure *ExpCCP* for all volume bins in the sample. Each volume bin corresponds to a 15 minutes on the wall clock *on average*. Panel (a) plots exposure level defined as the 99% VaR of aggregate loss in member accounts for the oncoming period (i.e., volume bin). Panel (b) plots the first difference of this series. Each shaded area corresponds to one month and wider areas therefore reflect more trading volume during the month.

returns otherwise. Bhanot et al. (2014) find that Greek yield spread increases are associated with negative abnormal returns on financial stocks throughout Europe. Beetsma et al. (2013) document spillover effects from the Greek yield spread to those of other European counties and Candelon, Sy, and Arezki (2011) find similar evidence when studying credit default swaps (CDS) on sovereign debt. We will return to this event when decomposing *ExpCCP* in Section 5.2. The bottom graph of Figure 1 plots exposure *changes* instead of levels. It shows that periods with high levels do not necessarily correspond to periods with disproportionate intraday increases. It is the latter that CPMI-IOSCO (2017) is particularly worried about when presenting its latest guidance on CCP risk management. The two peaks correspond to the following two idiosyncratic events:

1. At noon on April 22, 2010, Nokia announced earnings that were far below analyst expectations. Its share price dropped by about 15% in subsequent minutes. Volume jumped and remained high throughout the afternoon, 400% above what volume was in the morning of that day.

2. Shortly after market open on August 18, 2010, the world No.1 wind turbine maker Vestas posted a surprise second-quarter loss and unexpectedly cut its 2010 earnings outlook. The share price dropped by 21% in subsequent minutes on highly elevated volume.

We revisit the "Nokia event" when decomposing $\Delta ExpCCP$ in Section 5.1.

5.1 H1: The drivers of CCP exposure changes are different in the (right) tail.

Hypothesis 5.1 states essentially states that extremely large sudden increases in CCP exposure are different in nature than regular changes. As discussed in the hypothesis development section (Section 2), they are likely to reflect a jump in volatility and elevated trading. There might also be crowding if members all tilt their portfolio to the single risk factor at the heart of the turbulence (in the later part of the section, we explore a Nokia event to illustrate). These stand in contrast to "average" changes in CCP exposure that we conjecture mostly reflect member position changes due to trade.

To test the hypothesis, we decompose CCP exposure changes into various components for the full sample, for the top 100 increase, and for the top 10 increases (See Section 3.2 for details on the decomposition approach). Table 3 presents the decomposition results and yields the following insights. First, for the

Table 3: Decomposition of changes in CCP exposure. This table presents the composition of CCP exposure change for all changes and separately for the top 100 and top 10 changes. Panel A presents the decomposition in euro. Panel B presents the same decomposition but in percentages. The five components capture changes in security return volatilities (*RetVola*), security return correlations (*RetCorr*), the pricing level (*PrLevel*), outstanding member positions (*TrPosition*), and the extent of overlap in member positions (*TrCrowding*).

	Full sample	Top 100 $\Delta ExpCCP$	Top 10 $\Delta ExpCCP$
Panel A : CCP exposure change decomposition in euro			
RetVola	-636	6,056	45,920
RetCorr	-102	823	-2,899
PrLevel	-143	6,167	-6,091
TrPosition	19,734	58,247	82,307
TrCrowding	685	10,731	23,295
$\Delta ExpCCP$	19,538	82,023	142,532
Panel B: CCP exposure change decomposition in percentage			
RetVola	-3.3%	7.4%	32.3%
RetCorr	-0.5%	1.0%	-2.0%
PrLevel	-0.7%	7.5%	-4.3%
TrPosition	101.0%	71.0%	57.7%
TrCrowding	3.5%	13.1%	16.3%
$\Delta ExpCCP$	100.0%	100.0%	100.0%

full sample indeed member positions is the only component that explains position changes.

Second, when zooming in on the top 100 and top 10 changes, a different picture emerges. While position drops to 71.0% and 57.7% respectively, two other components, volatility and crowding, grow much more important. The volatility component makes up only -3.3% of the exposure change for the full sample but jumps to 7.4% and 32.2% for the top 100 and top 10 increases, respectively.[22] The crowding component is only 3.5% of the exposure changes for the full sample but jumps 13.1% and 16.3% the top 100 and top 10 increases, respectively.

Third, the price and correlation component remain small in the two subsamples. Overall, all of these findings support the hypothesis that extreme increases in CCP exposure are different in nature than overall average changes. Specifically, while average CCP exposure changes are close to completely driven by member position changes, extreme ones exhibit substantial contributions from volatility changes and increased position crowding across members.

In Appendix D we show that these findings are robust to changing the com-

[22]Note that percentages in this analysis can turn negative since they simply represent a component's contribution scaled by total changes in CCP exposure.

ponent sequencing, the estimate of the time-varying return covariance, and the sampling frequency. One notable result worth mentioning here is that for lower frequencies the difference between the full sample and the top 10 gets attenuated. This highlights the importance of monitoring changes in CCP exposure at high frequencies.[23]

To illustrate these general findings, we zoom in one of the two largest two CCP exposure increases and provide a diagnostic analysis. Panel (a) of Figure 2 graphically decomposes the exposure jump immediate following Nokia's disappointing announcement. A couple of features stand out. First, return volatility is by far the largest component: €0.37 million. Its effect is moderated some by the price-level component being negative: €-0.10 million. In other words, volatility spikes due to a large and immediate negative return on Nokia of about -15%, but relative volatility operates at a lower price level because of the negative return. It is the latter effect that is subsumed by the price-level component. Finally, the trade components all add to CCP exposure implying that on average traders are expanding their positions and their position-taking leads to more crowding. All these trade component however are dwarfed by the volatility component.

Panel (b) of Figure 2 zooms out and shows how CCP exposure built up throughout the day of the Nokia event. Its most salient feature is that while the volatility spike dominates exposure change in the volume bin after the event, it is only about a fifth of that day's exposure change. The reason is that volatility is a negligible component (i.e., no further strong changes in volatility) in the hours after the event, but trade components contribute a lot to CCP exposure changes in the afternoon.

Elevated volume in the afternoon turns out to be of the nature that traders expand their positions in the aftermath of the event, they do not reduce them. This might be due to diverging beliefs on how the Nokia events affects the company's fundamental value. There is also substantial crowding. Finally, there does not seem to be substantial position-taking *ahead* of the announcement as all components only start to contribute substantially after the announcement.

Perhaps the most important message of these Nokia results is that firm-specific shocks can have systemic impact through heightened CCP exposure. News that strikes like lightning causes volatility to spike and, more importantly, makes traders expand their position in such a way that there more concentration in their portfo-

[23] For completeness we also did these robustness analyses for the empirical results on the second and third hypothesis. Again, the results do not change qualitatively. To conserve space we decided to only provide these robustness results upon request.

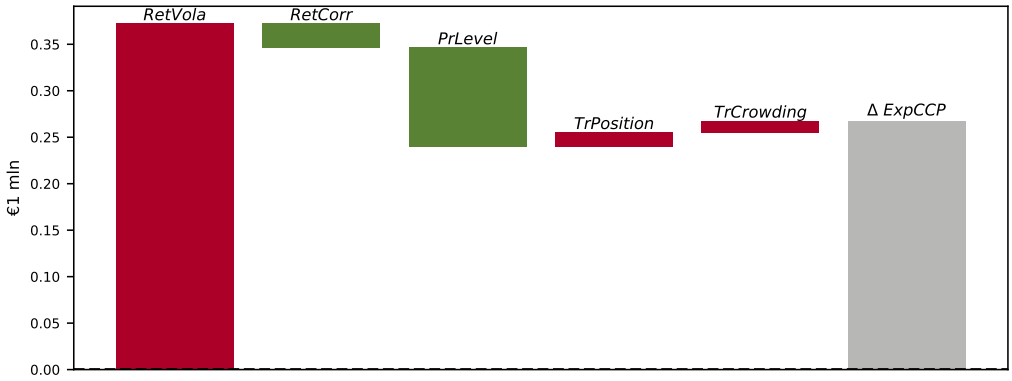

(a) Decomposition of Δ*ExpCCP* for bin 21 on April 22, 2010, 12:01:02 - 12:03:02

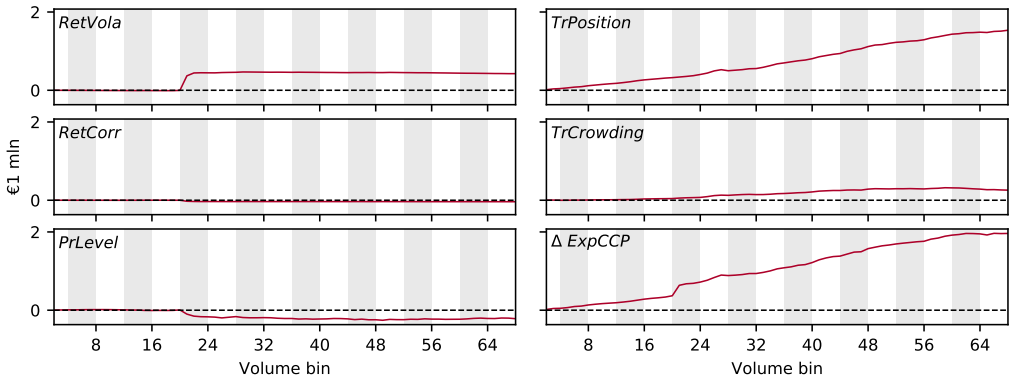

(b) Decomposition of Δ*ExpCCP* for all volume bins on April 22, 2010

Figure 2: Decomposition of an extreme CCP exposure increases: Nokia. At noon on April 22, Nokia announced disappointing earnings which caused the stock price to drop by 15% on elevated trading. CCP exposure rose steeply in the volume bin just after, being one of the two extreme exposure increases in the sample. Panel (a) decomposes this exposure change into five components: security return volatilities (*RetVola*), security return correlations (*RetCorr*), the pricing level (*PrLevel*), outstanding member positions (*TrPosition*), and the extent of overlap in member positions (*TrCrowding*). Panel (b) bottom panel zooms out and cumulates these components for the full day.

lios (i.e., crowding).

Table 4: Decomposition of CCP exposure across members and across stocks. This table presents the results of decomposing CCP exposures across members and across stocks, for the full sample and for subsamples with high levels. Various concentration measures are reported: the share of the member with the highest level, the five highest levels, and the 10 highest levels. The table further reports the Herfindahl-Hirschman Index.

	Full sample	Top 10% *ExpCCP*	Top 1% *ExpCCP*
Panel A: Decomposition of CCP exposure across traders			
Top 1 member	9.5%	14.8%	26.3%
Top 5 members	28.5%	35.2%	47.3%
Top 10 members	42.5%	48.6%	57.3%
Herfindahl-Hirschman Index (HHI)	0.031	0.048	0.088
Panel B: Decomposition of CCP exposure across stocks			
Top 1 stock	17.4%	22.2%	14.8%
Top 5 stocks	42.6%	44.1%	39.1%
Top 10 stocks	59.4%	59.4%	56.7%
Herfindahl-Hirschman Index (HHI)	0.075	0.124	0.048

5.2 H2: The structure of CCP exposure levels is different in the (right) tail.

The second hypothesis focuses on extremely large exposure *levels* as opposed to changes. Does one see evidence of elevated exposure concentration (i.e., crowding) either across members, across (combination of) stocks, or across both? Such finding would raise concerns about market conditions that are potentially prone to fire-sale dynamics. The analysis we perform in this subsection measure concentration in the tail and compares it to overall average levels. If there is such elevated concentration the decomposition across members and stocks will highlight where it originates.

To verify whether the structure of CCP exposure is different in the tail, we decompose exposure for the full sample and for the subsamples of the top 10% and the top 1% CCP exposure levels (see Section 3.3 for details on the decomposition).[24] The decomposition is done both across members and across stocks. We the compute the Herfindahl-Hirschman Index (HHI) along with shares of the largest 1, 5, and 10 contributors to measure the concentration level.

Table 4 reveals that indeed concentration seems elevated in the tail but only

[24]The reason for picking the top 10% here instead of the top 100 used in the previous subsection is that CCP exposure levels are very persistent as compared to exposure changes. The top 100 subsample is smaller than the top 10% one and, therefore, when used in the level analysis it would essentially point to the same period of time. The same argument applies to picking top 1% instead of top 10.

Table 5: Principal component analysis of member portfolio returns. This table uses principal component analysis to characterize the commonality in member portfolio returns for the full sample and for subsamples where either CCP exposure levels or changes are extreme. It reports the size of the first, the second, and the third principal component along with the sum of these three.

	Full sample	Top 10% *ExpCCP*	Top 1% *ExpCCP*
PC1	7.1%	20.3%	41.7%
PC2	5.0%	9.3%	8.3%
PC3	2.7%	5.6%	5.3%
PC1+PC2+PC3	14.8%	35.3%	55.4%

for members, not for individual stocks. For all three share measures (i.e., share of the top 1, 5, and 10 members) the concentration increases substantially from the full sample to the top 1% sample. For example, the share of the largest five members increases from 28.5% to 35.2% and 47.3% for the top 10% and top 1%, respectively. The HHI index shows a similar trend and increases from 0.031 to 0.048 and 0.088, respectively. There is no such trend in the corresponding numbers for the decomposition across individual stocks. The share of the top five members, for example, stays rather flat. It changes from 42.6% to 44.1% and 39.1% for the top 10% and top 1% exposure level, respectively.

The unchanged concentration for the decomposition across stocks does not preclude crowding in a particular *portfolio* of stocks. To study whether this is the case, we apply principal component analysis (PCA) on member portfolio returns for the full sample and both subsamples. Table 5 shows that there does appear to be elevated crowding when comparing the full sample with the two subsamples. It is strongest for the first principal component whose share in total variance increases from 7.1% in the full sample to 20.3% for the top 10% sample and 41.7% for the top 1% sample. As the extreme CCP exposures occur mostly in the Greek crisis period, it is likely that this components captures this macro event. To verify, we compute the correlation of PC1 with the local market index and find its correlation to be 0.41, 0.85, and 0.97 for the full sample and the two consecutive subsamples. Indeed, in these times of elevated exposure members appear to trade mostly the plain-vanilla market portfolio. The table further shows that there is a monotonic increase for PC2 and PC3 as well, but those increases are much more moderate in size.

Finally, to illustrate these results graphically Figure 3 plots the Herfindahl-Hirschman index for both cross-member and cross-stock decompositions (see Ta-

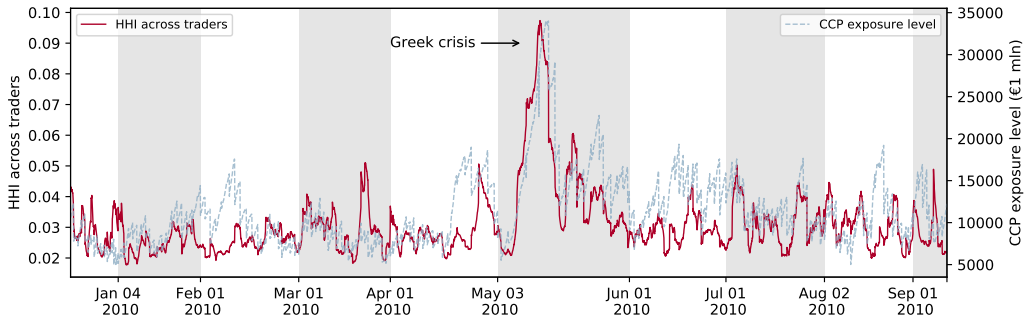

(a) Herfindahl-Hirschman Index (HHI) of decomposition across members

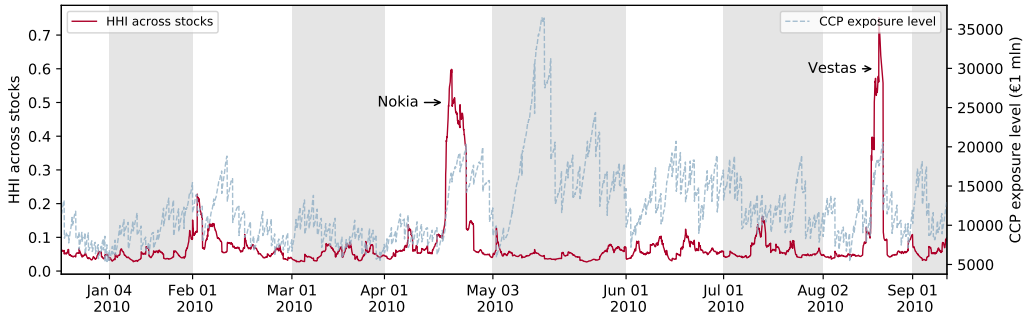

(b) Herfindahl-Hirschman Index (HHI) of decomposition across stocks

Figure 3: CCP exposure dispersion across members and across stocks. This figure plots the Herfindahl-Hirschman Index (HHI) of CCP exposure decomposed across members in Panel (a), and across stocks in Panel (b). It therefore tracks the level of concentration across time. The plots also plot CCP exposure levels (right y-axis).

Table 6: Decompositions CCP exposure across house and client accounts. Panel A decomposes CCP exposure across house and client accounts. Panel B shows the concentration of CCP exposure *within* each account type by means of the Herfindahl-Hirschman Index (HHI). Both panels consider the full sample and subsamples of the top 10% and the top 1% CCP exposure levels.

	Full sample	Top 10%	Top 1%
Panel A: Decomposition CCP exposure across account type			
Contribution by house accounts (%)	67.2%	67.6%	70.3%
Contribution by client accounts (%)	32.8%	32.4%	29.7%
Panel B: Concentration CCP exposure within account type			
Herfindahl-Hirschman Index (HHI) within house accounts	0.052	0.085	0.163
Herfindahl-Hirschman Index (HHI) within client accounts	0.070	0.077	0.085

ble 4). Panel (a) plots the cross-member index in solid red and overlays the CCP exposure level in dashed blue (using the second y-axis). It illustrates that highest concentrations are occur mostly in the Greek crisis period. Panel (b) plots the cross-stock index and, as expected, it stays rather flat at times where CCP exposure peaks, but interestingly it does exhibit peaks but these appear to occur at times of extreme level increases as analyzed in the previous subsection. The Nokia and Vestas events correspond with the salient peaks. Upon further inspection we unsurprisingly find that the concentration manifests itself in the stocks of Nokia and Vestas, respectively.

5.3 H3: The relative contribution of house accounts increases in the (right) tail.

The third hypothesis states that the relative contribution of house accounts is higher for extreme CCP exposure levels. This is potentially worrisome as clearing members are highly leveraged financial institutions.

Table 6 presents evidence largely rejecting the third hypothesis. The decomposition across house and client accounts in Panel A shows that house accounts contribute 67.2% to CCP exposure in the full sample. This contribution however almost does not change in top 10% subsample and increases only mildly to 70.3% in the top 1% subsample.

Panel B shows that in spite of the relative contribution of all house accounts combined being rather flat across subsamples, there is concentration *within* house accounts. The Herfindahl-Hirschman index computed based on each member's house account's share in total house accounts increases from 0.052 for the full

sample to 0.085 for the top 10% and 0.163 for the top 1%. The results suggest that in stressed markets the positions in the books of some clearing members expand while the positions of others shrink. This causes their total contribution to CCP exposure to remain unchanged, yet there is more concentration within the set of clearing members.

There appears to be no such pattern for client accounts whose collective contribution remains flat across the three samples but also the within-client concentration remains largely unchanged. The Herfindahl-Hirschman index is 0.070 for the full sample, 0.077 for the top 10% subsample, and 0.085 for the top 1% sample.

In sum, the significantly higher concentration within house accounts is potentially worrisome. Most clearing members are highly leveraged sell-side banks who, if trading for speculative reasons, might default on their position if they turn out to be on the wrong side of the bet. Given that they seem to crowd on the same (set of) risk factors, there might be multiple that are heavily under water on their bets at the same time. Admittedly, it is unlikely that they default on their equity trades, but if the same pattern holds true for CCPs that clear interest rate derivatives or CDS contracts, then such dynamic does become a systemic worry.

6 Conclusion

In summary, we test three hypotheses about the exposure a CCP has vis-à-vis its clearing members. All three hypotheses focus on tail events and whether or not the nature of CCP exposure changes in such cases. The academic literature has emphasized elevated concentration (i.e., crowding) in such stressed markets with a risk of fire-sale price dynamics.

We develop an approach for monitoring CCP exposure whereby both exposure *level* and exposure *changes* can be decomposed to identify the relative contribution of various factors. The empirical results confirm the hypothesized differences when comparing extreme CCP exposure levels or changes to the full sample. There indeed is more crowding in the tails. The hypothesized higher contribution by clearing member house accounts as opposed to client accounts did not find empirical support. However, *within* house accounts there is more concentration with few clearing members contributing a disproportionate amount of total house-account exposure.

Our findings suggest that CCP executives and regulators should monitor at high frequency with particular focus on tail events. Whether or not contingency planning is needed and if so, in what form, is for future research. We however

believe that the approach we developed is useful for monitoring CCP exposure at high frequencies. The decompositions allow for immediate diagnostic analysis. As all results are analytic thus avoiding heavy-duty simulations, the approach can be implemented in real-time. This we believe is an asset in today's extremely fast markets.

Appendix

A Decomposition of CCP exposure change

This section presents the various components that add up to CCP exposure change from $t-1$ to t:

$$\Delta ExpCCP_t = \underbrace{RetVola_t + RetCorr_t + PrLevel_t}_{\text{Price components}} + \underbrace{TrPosition_t + TrCrowding_t}_{\text{Trade components}}. \tag{18}$$

Price components. The three price components are:

$$\begin{aligned} RetVola_t =& f\left(D\left(\boldsymbol{D_{\Omega_t}}, R_{\Omega_{t-1}}, P_{t-1}, \tilde{N}_{t-1}\right), R\left(\boldsymbol{D_{\Omega_t}}, R_{\Omega_{t-1}}, P_{t-1}, \tilde{N}_{t-1}\right)\right) \\ & - f\left(D\left(D_{\Omega_{t-1}}, R_{\Omega_{t-1}}, P_{t-1}, \tilde{N}_{t-1}\right), R\left(D_{\Omega_{t-1}}, R_{\Omega_{t-1}}, P_{t-1}, \tilde{N}_{t-1}\right)\right), \end{aligned} \tag{19}$$

$$\begin{aligned} RetCorr_t =& f\left(D\left(D_{\Omega_t}, \boldsymbol{R_{\Omega_t}}, P_{t-1}, \tilde{N}_{t-1}\right), R\left(D_{\Omega_t}, \boldsymbol{R_{\Omega_t}}, P_{t-1}, \tilde{N}_{t-1}\right)\right) \\ & - f\left(D\left(D_{\Omega_t}, R_{\Omega_{t-1}}, P_{t-1}, \tilde{N}_{t-1}\right), R\left(D_{\Omega_t}, R_{\Omega_{t-1}}, P_{t-1}, \tilde{N}_{t-1}\right)\right), \text{ and} \end{aligned} \tag{20}$$

$$\begin{aligned} PrLevel_t =& f\left(D\left(D_{\Omega_t}, R_{\Omega_t}, \boldsymbol{P_t}, \tilde{N}_{t-1}\right), R\left(D_{\Omega_t}, R_{\Omega_t}, \boldsymbol{P_t}, \tilde{N}_{t-1}\right)\right) \\ & - f\left(D\left(D_{\Omega_t}, R_{\Omega_t}, P_{t-1}, \tilde{N}_{t-1}\right), R\left(D_{\Omega_t}, R_{\Omega_t}, P_{t-1}, \tilde{N}_{t-1}\right)\right). \end{aligned} \tag{21}$$

Trade components. The two trade components are:

$$\begin{aligned} TrPosition_t =& f\left(D\left(D_{\Omega_t}, R_{\Omega_t}, P_t, \boldsymbol{\tilde{N}_t}\right), R\left(D_{\Omega_t}, R_{\Omega_t}, P_t, \tilde{N}_{t-1}\right)\right) \\ & - f\left(D\left(D_{\Omega_t}, R_{\Omega_t}, P_t, \tilde{N}_{t-1}\right), R\left(D_{\Omega_t}, R_{\Omega_t}, P_t, \tilde{N}_{t-1}\right)\right) \text{ and} \end{aligned} \tag{22}$$

$$\begin{aligned} TrCrowding_t =& f\left(D\left(D_{\Omega_t}, R_{\Omega_t}, P_t, \tilde{N}_t\right), R\left(D_{\Omega_t}, R_{\Omega_t}, P_t, \boldsymbol{\tilde{N}_t}\right)\right) \\ & - f\left(D\left(D_{\Omega_t}, R_{\Omega_t}, P_t, \tilde{N}_t\right), R\left(D_{\Omega_t}, R_{\Omega_t}, P_t, \tilde{N}_{t-1}\right)\right). \end{aligned} \tag{23}$$

B Example of CCP exposure change analysis

Table 7 summarily presents the insights a decomposition of CCP exposure changes can generate based on a very simple example. Suppose there are four agents ($A1$, $A2$, $A3$, $A4$) and two securities ($S1$ and $S2$) that trade at a price of one with returns that are standard normal and mutually independent at least at the beginning of

time. All agents start with a zero position in the securities. To illustrate real-time CCP exposure monitoring, we consider a sequence of events occurring in subsequent periods. We compute CCP exposure change for each period and present its decomposition. This controlled setting serves to familiarize with the approach before implementing it on real data.

The first two columns describe the sequence of events. CCP exposure is computed at each snapshot based on the loss distribution for the oncoming period. In some cases, events are illustrated by horizontal arrows that correspond to positions in the first security. Arrows that point right denote long positions. Arrows left denote short positions. Vertical arrows correspond to positions in the second security. Arrows up denote long positions. Arrows down denote short positions. The remaining columns present CCP exposure, its change over the period just ended, and the decomposition into the five factors. These changes and decompositions are discussed below.

- $t = 0$. CCP exposure is 0 for the simple reason that none of agents has a position.

- $t = 1$. *A1* has entered a one unit long position on *S1* and *A2* is on the opposite side of that trade. CCP exposure becomes 2.3. The decomposition shows that 2.9 is due to expanded positions (*TrPosition*) and the crowding component is -0.6 (*TrCrowding*). The reason for this negative crowding term is simply that in this case the members have taken the opposite site of the same trade and their portfolio returns are thus perfectly negatively correlated.

- $t = 2$. *A3* has entered a one unit long position in *S2* with *A4* has taken the short side. CCP exposure increases by 1.4 units to 3.7. The decomposition shows a positive *TrPosition* of 1.8 and a negative *TrCrowding* of -0.4. The positive position risk is because the new trade leads to larger positions. Furthermore, the new trade between *A3* and *A4* is in *S2* and therefore orthogonal to the positions between *A1* and *A2*. In other words, the new trade between *A3* and *A4* lowers the correlations between member portfolio returns. Hence, there is less crowding now than before.

- $t = 3$. The return volatility of *S1* has increased from 1 to 2. CCP exposure increases by 2.0 to 5.7. The decomposition indeed attributes it to the volatility component (*RetVola*).

Table 7: Simple example to illustrate the decomposition of CCP exposure changes. This example illustrates how the OFAT decomposition approach identifies the different components in CCP exposure changes. There are four agents (*A1*, *A2*, *A3*, *A4*) and two securities (*S*1, *S*2). Arrows denote positions in these securities. Arrows right and left illustrate long and short positions in *S*1, arrows up and down illustrate long and short positions in *S*2. Red dashed arrows correspond to new trades in the interval. CCP exposures are computed with $\alpha = 2.5$, which is the calibrated value based on our real-world sample (see Section 4.2).

t	Trades/changes	$ExpCCP_t$	$\Delta ExpCCP_t$ =	$RetVola_t$ +	$RetCorr_t$ +	$PrLevel_t$ +	$TrPosition_t$ +	$TrCrowding_t$
0	$\sigma_1 = \sigma_2 = 1, \rho = 0$, $p_1 = p_2 = 1$.	0.0	0.0	0.0	0.0	0.0	0.0	0.0
1		2.3	2.3	0.0	0.0	0.0	2.9	-0.6
2	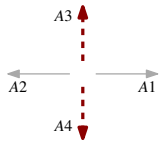	3.7	1.4	0.0	0.0	0.0	1.8	-0.4
3	Volatility changes from $\sigma_1 = \sigma_2 = 1$ to $\sigma_1 = 2, \sigma_2 = 1$.	5.7	2.0	2.0	0.0	0.0	0.0	0.0
4	Return correlation changes from $\rho = 0$ to $\rho = 0.5$.	6,0	0.3	0.0	0.3	0.0	0.0	0.0
5	Price level changes from $p_1 = p_2 = 1$ to $p_1 = 0.5, p_2 = 1$.	3.9	-2.1	0.0	0.0	-2.1	0.0	0.0
6	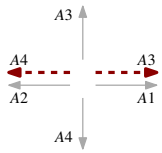	6.7	2.8	0.0	0.0	0.0	1.5	1.3
7	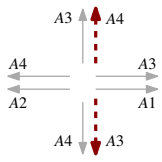	4.6	-2.1	0.0	0.0	0.0	-2.0	-0.1

- $t = 4$. The correlation between the returns of *S1* and *S2* increases from 0 to 0.5. CCP exposure increases by 0.3 to 6.0. The decomposition assigns it to the correlations component (*RetCorr*).

- $t = 5$. The price of *S1* drops from 1 to 0.5. CCP exposure drops by 2.1 which is completely assigned to the price level (*PrLevel*). This is simply the result of volatility being defined in relative terms. If it does not change, but the price level drops then the VaR expressed in *dollars* drops.

- $t = 6$. *A3* trades again with *A4* but this time he enters a one-unit long position in *S1* where *A4* takes the short side. CCP exposure increases by 2.8 to 6.7. Positions now crowd on the risk factor *S1*. The decompositions assigns 1.3 of the increase to *TrCrowding* and the remaining 1.5 to *TrPosition*.

- $t = 7$. *A3* and *A4* effectively undo their first trade by entering a reverse trade. In this reverse trade *A3* is long one unit of *S2* and *A4* is short one unit. CCP exposure declines by 2.1 to 4.6. The decomposition shows that most of the decrease is due to a reduction in outstanding (net) positions (i.e., the drop is largely assigned to *TrPosition*). This event shows that trade does not necessarily imply more exposure, it could *reduce* exposure when, after the trade, positions shrink. Note that combining $t = 6$ and $t = 7$ the *size* of trade positions have not changed — members are long or short the same amount of risk — but CCP exposure has increased due position crowding.

In summary, decomposition of CCP exposure changes generates insight into the drivers of these changes. *TrPosition* picks up whether new trades extend or reverse legacy positions. *TrCrowding* captures the correlation of member portfolio returns. *RetVola*, *RetCorr*, and *PrLevel* identify exposure changes due to changes in the volatility of returns, their correlations, and price levels, respectively.

C Decomposition of CCP exposure across securities

ExpCCP being homogeneous of degree one in $\omega_k, k = 1, 2, \ldots, I$ yields:

$$ExpCCP = \sum_i \omega_k \left(\frac{\partial}{\partial \omega_k} ExpCCP \right). \tag{24}$$

The contribution of security k therefore is:

$$\begin{aligned} ExpCCP_k &= \sum_{i,j} \omega_k \left(\frac{\partial}{\partial \omega_k} ExpCCP \right) \\ &= \sum_j \sqrt{\frac{1}{2\pi}} \frac{B_{jj}}{2\sigma_j} + \\ &\quad + \frac{\alpha}{2\text{std}A} \sum_{i,j} \left(\frac{\pi - 1}{2\pi} \right) \left(M' \left(\rho_{ij} \right) B_{ij} + \frac{\sqrt{1 - \rho_{ij}^2} - 1}{\pi - 1} \left(\frac{\sigma_j}{2\sigma_i} B_{ii} + \frac{\sigma_i}{2\sigma_j} B_{jj} \right) \right) \end{aligned} \tag{25}$$

where

$$B_{ij} = n_i' \frac{\partial \Omega}{\partial \omega_k} n_j. \tag{26}$$

Note that each element ω_{ij} of the covariance matrix Ω can be written as $\rho_{ij}\omega_i\omega_j$ where ρ_{ij} denotes the elements of the accompanying correlation matrix. This should clarify what the result of the partial derivative $\frac{\partial \Omega}{\partial \omega_k}$ is.

D Robustness checks

D.1 Alternative sequencing in exposure change decomposition

The decomposition of CCP exposure change presented in Table 3 and discussed in Section 5.1 critically depends on the sequencing of the various components. To verify how robust the decomposition results are to alternative sequences, we redo the analysis across all possible alternatives. As the components sort into two groups that are naturally preserved in the ordering, we end up with doing the decomposition for $2 \times 3! \times 2! = 24$ possible sequences.

The results in Table 8 show that the decomposition results appear robust. The table reports the mean, the lower and the upper bound of each component's contribution across all 24 sequences. The distance between the lower and upper bounds seems small as it only a few percentage points for the relative shares reported in Panel B, never exceeding six points. The key observations in the main text all hold up: The position component dominates all other for the full sample, but volatility and crowding become progressively more important when considering only the top-100 and top-10 exposure changes.

Table 8: Decomposition of exposure change for alternative component sequences. This table presents the mean and, in brackets, the lower and the upper bound of the (relative) share of components across alternative sequences of the various components. It serves as a robustness check for Table 3 which is based on a particularly economically motivated sequence. The price and trade variables are kept together as a group so the number of sequences considered is $2 \times 3! \times 2! = 24$.

	Full sample	Top 100 $\Delta ExpCCP$	Top 10 $\Delta ExpCCP$
	Panel A : CCP exposure change decomposition in euro		
RetVola	-637	5,995	45,054
	(-646, -628)	(5,586, 6,415)	(4,1252, 4,8940)
RetCorr	-102	864	-2,649
	(-105, -99)	(809, 917)	(-3,216, -2,107)
PrLevel	-143	6,335	-4,335
	(-150, -136)	(6,098, 6,564)	(-6,632, -2,094)
TrPosition	20,301	59,325	83,879
	(19737, 20,865)	(58,033, 60,631)	(80,707, 87,171)
TrCrowding	118	9,504	20,584
	(-446, 683)	(8,298, 10,723)	(18,009, 23,280)
$\Delta ExpCCP$	19,538	82,023	142,532
	Panel B: CCP exposure change decomposition in percentage		
RetVola	-3.3%	7.3%	31.6%
	(-3.3%, -3.2%)	(6.8%, 7.8%)	(28.9%, 34.3%)
RetCorr	-0.5%	1.1%	-1.9%
	(-0.5%, -0.5%)	(1.0%, 1.1%)	(-2.3%, -1.5%)
PrLevel	-0.7%	7.7%	-3.0%
	(-0.8%, -0.7%)	(7.4%, 8.0%)	(-4.7%, -1.5%)
TrPosition	103.9%	72.3%	58.8%
	(101%, 106.8%)	(70.8%, 73.9%)	(56.6%, 61.2%)
TrCrowding	0.6%	11.6%	14.4%
	(-2.3%, 3.5%)	(10.1%, 13.1%)	(12.6%, 16.3%)
$\Delta ExpCCP$	100.0%	100.0%	100.0%

Table 9: Decomposition of exposure change for rolling-window estimate of return covariance. This table repeats the baseline exposure change decomposition result reported in Table 3 and adds the decomposition result when, instead of an EWMA estimate of the return covariance, one uses a rolling-window estimate based on 50 days (same as burn-in period used for EWMA).

	EWMA estimate of Cov(R)			Rolling-window estimate of Cov(R)		
	Full sample	Top 100	Top10	Full sample	Top 100	Top10
	Panel A : CCP exposure change decomposition in euro					
RetVola	-636	6,056	45,920	-429	3,911	30,171
RetCorr	-102	823	-2,899	12	496	-922
PrLevel	-143	6,167	-6,091	-145	5,455	-2,255
TrPosition	19,734	58,247	82,307	19,705	58,676	76,311
TrCrowding	685	10,731	23,295	684	11,737	20,423
$\Delta ExpCCP$	19,538	82,023	142,532	19,826	80,276	123,728
	Panel B: CCP exposure change decomposition in percentage					
RetVola	-3.3%	7.4%	32.2%	-2.2%	4.9%	24.4%
RetCorr	-0.5%	1.0%	-2.0%	0.1%	0.6%	-0.7%
PrLevel	-0.7%	7.5%	-4.3%	-0.7%	6.8%	-1.8%
TrPosition	101.0%	71.0%	57.7%	99.4%	73.1%	61.7%
TrCrowding	3.5%	13.1%	16.3%	3.4%	14.6%	16.5%
$\Delta ExpCCP$	100.0%	100.0%	100.0%	100.0%	100.0%	100.0%

D.2 Covariance matrix

The exposure change decomposition analysis presented in Table 3 relies on a EWMA estimate of the covariance matrix of returns. To verify whether the results are robust we redo the analysis with a rolling-window estimate of return covariance. For the length of the window we picked the burn-in period used for EWMA (i.e., 50 days). We have considered other alternatives such as parametric estimation of the time-varying covariance matrix. The most natural candidate is multivariate GARCH but implementation is infeasible given the large covariance matrix that needs to be estimated: 242×242. We therefore stick to a parameter-free rolling-window estimate.

Table 9 repeats results Table 3 and adds the ones based on a rolling-window estimate of the covariance of returns. The results are very similar. Importantly, the key observations in the main text all hold up: The position component dominates all other for the full sample, but volatility and crowding become progressively more important when considering only the top-100 and top-10 exposure changes.

Table 10: Decomposition of exposure change for different frequencies. This table repeats the decomposition of CCP exposure change presented Table 3 and adds the same results but for different frequencies. The baseline result is based on having, on average, 34 volume bins per day which corresponds to 15-minute intervals. The added frequencies are 17 and 8 and therefore correspond to 30-minute and 1-hour intervals, respectively.

	Baseline: 34 bins per day (~15-minute intervals)		17 bins per day (~30 minutes intervals)		8 days per day (~1 hour intervals)	
	Full sample	Top 10	Full sample	Top 10	Full sample	Top 10
	Panel A : CCP exposure change decomposition in euro					
RetVola	-636	45,920	-1,734	67,879	-4,933	180,877
RetCorr	-102	-2,899	-138	9,580	-94	17,106
PrLevel	-143	-6,091	-395	-1,769	-1,627	-46,388
TrPosition	19,734	82,307	55,947	211,300	178,057	539,365
TrCrowding	685	23,295	2,016	38,341	7,696	113,184
$\Delta ExpCCP$	19,538	142,532	55,695	325,333	179,100	804,145
	Panel B: CCP exposure change decomposition in percentage					
RetVola	-3.3%	32.3%	-3.1%	20.9%	-2.8%	22.5%
RetCorr	-0.5%	-2.0%	-0.2%	2.9%	-0.1%	2.1%
PrLevel	-0.7%	-4.3%	-0.7%	-0.5%	-0.9%	-5.8%
TrPosition	101.0%	57.7%	100.5%	64.9%	99.4%	67.1%
TrCrowding	3.5%	16.3%	3.6%	11.8%	4.3%	14.1%
$\Delta ExpCCP$	100.0%	100.0%	100.0%	100.0%	100.0%	100.0%

D.3 Frequencies

Is high-frequency analysis important for the decomposition results presented in Table 3? Note that the volume bins were chosen such that, on average, they span fifteen minutes. A higher frequency is computationally feasible but economically impossible as "microstructure noise" start to bias return covariance estimates (Andersen et al., 2003). Lower frequency, however, is possible and in this section we redo the decomposition based on volume bins that, on average, span 30 minutes or a full hour.

Table 10 presents the results but only reports full-sample and top-10 decompositions for space considerations. The table shows that the main takeaway of this analysis remains unaffected: the position component dominates in the full sample, but volatility and crowding become important in top 10 subsample. These results however become attenuated when the analysis is done at lower frequencies. The contribution of volatility and crowding drops in the top 10 subsample. This result testifies to the importance of high frequency analysis of CCP exposure changes. Market turbulence caused by a sudden volatility spike and concurrent trading that leads to crowding occur in short-lived periods in today's fast markets.

References

Acharya, Viral and Alberto Bisin. 2014. "Counterparty Risk Externality: Centralized Versus Over-The-Counter Markets." *Journal of Economic Theory* 149:153–182.

Amini, Hamed, Damir Filipović, and Andreea Minca. 2015. "Systemic risk and central clearing counterparty design." *Swiss Finance Institute Research Paper* (13-34).

Andersen, Torben G, Tim Bollerslev, Francis X Diebold, and Paul Labys. 2003. "Modeling and forecasting realized volatility." *Econometrica* 71 (2):579–625.

Ané, Thierry and Hélyette Geman. 2000. "Order flow, transaction clock, and normality of asset returns." *The Journal of Finance* 55 (5):2259–2284.

Beetsma, Roel, Massimo Giuliodori, Frank De Jong, and Daniel Widijanto. 2013. "Spread the news: The impact of news on the European sovereign bond markets during the crisis." *Journal of International Money and Finance* 34:83–101.

Benos, Evangelos, Richard Payne, and Michalis Vasios. 2016. "Centralized trading, transparency and interest rate swap market liquidity: evidence from the implementation of the Dodd-Frank Act." Staff working paper no. 580, Bank of England.

Bhanot, Karan, Natasha Burns, Delroy Hunter, and Michael Williams. 2014. "News spillovers from the Greek debt crisis: Impact on the Eurozone financial sector." *Journal of Banking & Finance* 38:51–63.

Biais, Bruno, Florian Heider, and Marie Hoerova. 2016. "Risk-Sharing or Risk-Taking? Counterparty Risk, Incentives, and Margins." *Journal of Finance* 71:1669–1698.

Bignon, Vincent and Guillaume Vuillemey. 2016. "The Failure of a Clearinghouse: Empirical Evidence." Manuscript, HEC Paris.

Bliss, Robert and Robert Steigerwald. 2006. "Derivatives clearing and settlement: A comparison of central counterparties and alternative structures." *Manuscript* .

Bollerslev, Tim. 1990. "Modelling the coherence in short-run nominal exchange rates: a multivariate generalized ARCH model." *The review of economics and statistics* :498–505.

Brunnermeier, Markus K and Lasse H Pedersen. 2009. "Funding liquidity and market liquidity." *Review of Financial Studies* 22 (2201-2238):6.

Candelon, Bertrand, Mr Amadou NR Sy, and Mr Rabah Arezki. 2011. *Sovereign rating news and financial markets spillovers: Evidence from the European debt crisis*. 11-68. International Monetary Fund.

Capponi, Agostino, Wan-Schwin Allen Cheng, and Sriram Rajan. 2014. "Systemic risk: The dynamics under central clearing." *Available at SSRN* .

Clark, Peter K. 1973. "A subordinated stochastic process model with finite variance for speculative prices." *Econometrica: journal of the Econometric Society* :135–155.

CPMI-IOSCO. 2012. "Principles for Financial Market Infrastuctures." Manuscript, CPMI-IOSCO.

———. 2017. "Resilience and recovery of central counterparties (CCPs): Further guidance on the PFMI." Final report, CPMI-IOSCO.

Crego, Julio A. 2019. "Why Does Public News Augment Information Asymmetries." Manuscript, Tilburg University.

Cruz Lopez, Jorge, Jeffrey Harris, Christophe Hurlin, and Christophe Perignon. 2016. "CoMargin." *Journal of Financial and Quantitative Analysis* forthcoming.

Daniel, Cuthbert. 1973. "One-at-a-time plans." *Journal of the American statistical association* 68 (342):353–360.

Duffie, Darrell, Martin Scheicher, and Guillaume Vuillemey. 2015. "Central clearing and collateral demand." *Journal of Financial Economics* 116 (2):237–256.

Duffie, Darrell and Haoxiang Zhu. 2011. "Does a Central Clearing Counterparty Reduce Counterparty Risk." *The Review of Asset Pricing Studies* 1:74–95.

Easley, David, Marcos M López de Prado, and Maureen O'Hara. 2012. "Flow toxicity and liquidity in a high-frequency world." *The Review of Financial Studies* 25 (5):1457–1493.

EC. 2010. "The European Stabilization Mechanism." Memo/10/173, European Commission.

ECB. 2010. "ECB decides on measures to address severe tensions in financial markets." Press release, European Central Bank.

Engle, Robert. 2002. "Dynamic conditional correlation: A simple class of multivariate generalized autoregressive conditional heteroskedasticity models." *Journal of Business & Economic Statistics* 20 (3):339–350.

Fontaine, Jean Sebastien, Hector Perez-Saiz, and Joshua Slive. 2014. "How Should Central Counterparty Clearing Reduce Risk? Collateral Requirements and Entry Restrictions." Manuscript, Bank of Canada.

Glasserman, Paul, Ciamac C Moallemi, and Kai Yuan. 2015. "Hidden illiquidity with multiple central counterparties." *Operations Research* .

Gromb, Denis and Dimitri Vayanos. 2002. "Equilibrium and welfare in markets with financially constrained arbitrageurs." *Journal of financial Economics* 66 (2-3):361–407.

Hansen, Peter R and Asger Lunde. 2006. "Realized variance and market microstructure noise." *Journal of Business & Economic Statistics* 24 (2):127–161.

Huang, Wenqian. 2019. "Central counterparty capitalization and misaligned incentives." BIS working papers, Bank for International Settlements.

Hull, John and Alan White. 1998. "Value at risk when daily changes in market variables are not normally distributed." *Journal of derivatives* 5:9–19.

IMF. 2010. "Global Financial Stability Report: Meeting New Challenges to Stability and Building a Safer System."

Jones, C.M., G. Kaul, and M.L. Lipson. 1994. "Information, Trading, and Volatility." *Journal of Financial Economics* 36:127–154.

Jones, Robert A. and Christophe Perignon. 2013. "Derivatives Clearing, Default Risk and Insurance." *Journal of Risk and Insurance* 80:373–400.

Khandani, Amir E and Andrew W Lo. 2007. "What happened to the quants in August 2007?" *Journal of investment management* 5 (4):29.

———. 2011. "What happened to the quants in August 2007? Evidence from factors and transactions data." *Journal of Financial Markets* 14 (1):1–46.

Kim, Oliver and Robert E. Verrecchia. 1994. "Market Liquidity and Volume around Earnings Announcements." *Journal of Accounting and Economics* 17:41–67.

Koeppl, Thorsten, Cyril Monnet, and Ted Temzelides. 2012. "Optimal Clearing Arrangements for Financial Trades." *Journal of Financial Economics* 103:189–203.

Kyle, Albert S and Anna A Obizhaeva. 2016. "Market microstructure invariance: Empirical hypotheses." *Econometrica* 84 (4):1345–1404.

———. 2019. "Market microstructure invariance: A dynamic equilibrium model." *Anna A., Market Microstructure Invariance: A Dynamic Equilibrium Model (January 31, 2019)* .

Loon, Yee Cheng and Zhaodong Ken Zhong. 2014. "The impact of central clearing on counterparty risk, liquidity, and trading: Evidence from the credit default swap market." *Journal of Financial Economics* 112:91–115.

———. 2016. "Does Dodd-Frank affect OTC transaction costs and liquidity? Evidence from real-time CDS trade reports." *Journal of Financial Economics* 119 (3):645–672.

Menkveld, Albert J. 2016. "Systemic risk in central clearing: Should crowded trades be avoided?" *Manuscript* .

———. 2017. "Crowded positions: An overlooked systemic risk for central clearing parties." *The Review of Asset Pricing Studies* 7 (2):209–242.

Menkveld, Albert J., Emiliano Pagnotta, and Marius A. Zoican. 2015. "Does Central Clearing Affect Price Stability? Evidence from Nordic Equity Markets." Manuscript, Imperial College.

Mink, Mark and Jakob De Haan. 2013. "Contagion during the Greek sovereign debt crisis." *Journal of International Money and Finance* 34:102–113.

Park, Yang-Ho and Nicole Abruzzo. 2016. "An empirical analysis of futures margin changes: determinants and policy implications." *Journal of Financial Services Research* 49 (1):65–100.

Preis, Tobias, Dror Y. Kenett, Dirk Helbing, and Eshel Ben-Jacob. 2012. "Quantifying the Behavior of Stock Correlations Under Market Stress." *Scientific Reports (a Nature research journal)* 2:1–5.

Shleifer, Andrei and Robert W Vishny. 1997. "The limits of arbitrage." *The Journal of Finance* 52 (1):35–55.

Stein, Jeremy C. 2009. "Presidential address: Sophisticated investors and market efficiency." *The Journal of Finance* 64 (4):1517–1548.

Wagner, Wolf. 2011. "Systemic Liquidation Risk and the Diversity–Diversification Trade-Off." *The Journal of Finance* 66 (4):1141–1175.